Injected Current and Quantum Transmission Coefficient in Low Schottky Barriers: WKB and Airy Approaches

Raúl Rengel, Elena Pascual, and María J. Martín

***Abstract*—An exact solution of the quantum transmission coefficient has been obtained by using an Airy-transfer-matrix formalism to solve Schrödinger equation. The procedure is applied to the calculation of the transmission coefficient in reverse-biased low Schottky diodes. The barrier profiles are given by Monte Carlo device simulations. As compared to the exact calculation, results indicate that injected current is much exacerbated when considering Wentzel–Kramers–Brillouin (WKB) approach or when neglecting quantum mechanical reflections for energies over the potential barrier. However, WKB could reasonably predict the total current if properly modifying the model parameters. Influence of barrier lowering is also discussed.**

***Index Terms*—Airy functions, metallic source/drain, quantum transmission coefficient, Schottky barriers (SBs), semiconductor device modeling, Wentzel–Kramers–Brillouin (WKB) approach.**

I. Introduction

In the last years, the replacement of source/drain junctions in MOSFETs by low Schottky barrier (SB) metallic contacts is receiving a lot of attention as a solution to some of the roadblocks identified in the International Technology Roadmap for Semiconductors roadmap [1]–[3]. Accurate modeling of transport processes in such structures has therefore become the subject of important consideration. Most models, including commercial simulators, implement tunnel injection by considering the Wentzel–Kramers–Brillouin (WKB) approach [4]–[6]. Nevertheless, this approach is valid only for smoothly varying potentials, which may not be the case of SB junctions. Moreover, it neglects quantum mechanical reflections (QRs) for the thermoionic range of energies (and also for tunneling energies once that the turning point is crossed). Direct solution of Schrödinger equation is therefore required in order to obtain a correct quantum transmission coefficient (TC): the Airy-transfer-matrix (ATM) method has been successfully employed to this end in the field of multibarrier structures and superlattices [7]–[9]. Regarding silicon SB devices, a remarkable effort was carried out by Winstead and Ravaioli [10] by implementing the ATM in a 2-D Monte Carlo simulator for the study of SB MOSFETs. However, in that work the quantitative importance of QR for thermoionic current was not tackled and also no comparison was made to WKB results. Two recent papers [11] and [12] have also discussed ATM in silicon SB-MOSFETs. Nevertheless, only one transfer matrix is considered, which makes the model not suited to evaluate the TC in nonlinear barriers; secondly, the barrier width is determined by the turning point where the energy equals the potential, thus neglecting QR from the region where the impinging electron energies surpass the potential. Finally, an erroneous definition of the wave vector ([11, eq. 11] and [12, eq. 10]) combined with an incomplete derivative of Airy functions yields a TC in the right order of magnitude, but intrinsically inaccurate.

Therefore, the exact evaluation of the error induced by WKB approach in Schottky junctions remains an open question. In this letter, we present the results obtained using an ATM approach (and their comparison with WKB results) for the TC and injected current in a reverse-biased low-SB diode. The influence of QR and barrier lowering (BL) is also discussed.

Manuscript received September 26, 2006. This work was supported by the European Commission and the Consejería de Educación y Cultura de la Junta de Castilla y León under Research Projects METAMOS (IST-016677) and SA008B05, respectively. The review of this letter was arranged by Editor E. Sangiorgi.

The authors are with the Applied Physics Department of the Universidad de Salamanca, 37008 Salamanca, Spain (e-mail: raulr@usal.es).

Digital Object Identifier 10.1109/LED.2006.889511

II. ATM Approach and Simulated Structure

The ATM approach proceeds as follows [7]–[10]: The potential barrier is divided into a number of sections, and a linear interpolation for the potential is considered between each pair of the resulting nodes. By applying the continuity of the wave functions and their derivatives at each node, the relationship between the wave function coefficients of the incident and transmitted waves is obtained through the multiplication of a set of 2 × 2 matrices which include Airy functions and their derivatives in real space. In this way, the transmission coefficient as a function of the incident energy is given as

$$\mathrm{TC}(E_{\mathrm{inc}}) = \frac{|\Psi_{\mathrm{transmitted}}|^2}{|\Psi_{\mathrm{incident}}|^2} \cdot \frac{m_m^* k_{\mathrm{sc}}}{m_{\mathrm{sc}}^* k_m} \tag{1}$$

Ψ represents the wave functions, m_m^* and m_{sc}^* are the effective masses for the metal and the semiconductor and k_m and k_{sc} are the corresponding wave vectors. For the sake of simplicity, we have considered the same effective mass in the metal and in the semiconductor, 0.26 m_0. Most models follow this approach (see, i.e., [4], [5], [11], and [12]); in the absence of known values of the effective mass in the metal or silicide, another possibility is to consider m_m^* as a fitting parameter, as in [10]. In our main results the total barrier width is considered in the ATM calculations. However, one might think about using the width determined by the turning point (where $qV(x) = E_{\mathrm{inc}}$, $V(x)$ being the potential). In this alternative case, QR for energies

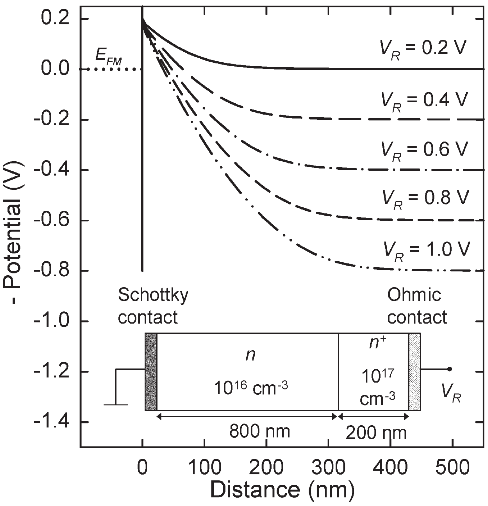

Fig. 1. Potential barrier profiles as a function of the longitudinal distance for V_R ranging from 0.2 to 1.0 V. The scheme of the Monte Carlo Schottky diode under study is shown at the bottom.

over the potential barrier would be neglected, which is physically incorrect. Anyway, we have additionally computed TC also in this way (from now on, we will refer to this possibility as "ATM without QR") in order to compare with the complete ATM results and discuss the contribution of QR. To determine the TC through WKB approach, the usual equations have been considered (see, i.e., [4] and [5]). The validity of our WKB and ATM calculations has been corroborated by comparison to the results for several barriers from the literature [7]. Once that the TC is determined by using WKB and ATM approaches, the injected current density can be obtained as [4], [13]

$$J_{\mathrm{inj}} = \frac{A^* T}{K_B} \int_0^{\infty} \mathrm{TC}(\xi) f_m(\xi) \left(1 - f_{\mathrm{sc}}(\xi)\right) d\xi \qquad (2)$$

f_m and f_{sc} being the Fermi–Dirac distribution functions in the metal and in the semiconductor, A^* Richardson's constant (240 $\mathrm{A \cdot cm^2 \cdot K^{-1}}$ [14]), T the temperature and K_B Boltzmann's constant. In the results shown, the zero level for the energies is the Fermi level in the metal.

In order to take into account a realistic SB profile, we carried out Monte Carlo simulations of the diode structure shown at the bottom of Fig. 1. A barrier to electrons equal to 0.2 eV is considered. The doping of the n region equals 10^{16} cm^{-3}, and an ohmic contact adjacent to an n^+ region is placed in order to apply the reverse voltage (V_R). The 1-D Monte Carlo simulator is described in [15]. The size of the cells is 1 nm, and approximately 25 000 superparticles have been simulated. V_R ranges from 0.2 to 1.0 V.

III. Results and Discussion

Fig. 1 shows the results for the barrier potential profile as a function of the distance (obtained by the average of the instantaneous potential determined solving self-consistently Poisson equation in the 1-D Monte Carlo kernel) for several values of V_R. The results of the TC obtained with the ATM method are shown in Fig. 2(a). As it can be observed, as V_R is increased,

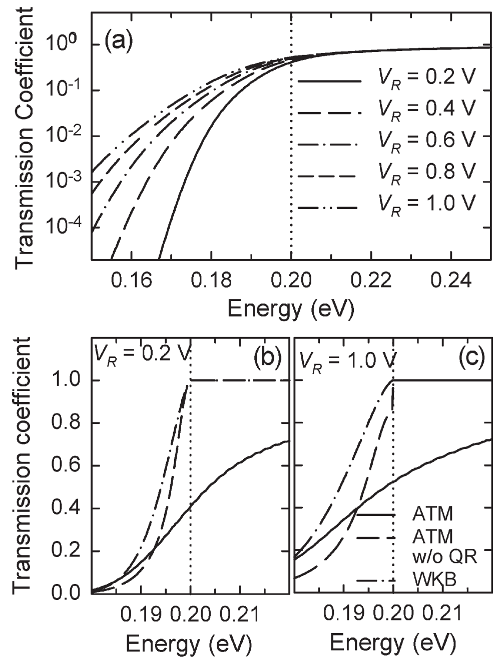

Fig. 2. Quantum transmission coefficient determined with the ATM method as a function of energy (a) and comparison between the results with complete ATM (solid lines), ATM without quantum reflections (dashed lines) and WKB (dash-dotted lines) for $V_R = 0.2$ V (b) and $V_R = 1.0$ V (c). The barrier height $q\phi_B$ is shown as a reference (vertical dotted lines).

the TC values increase for all energies below the barrier height $q\phi_B$ and some mV above, as it corresponds to the fact that the barrier gets sharper (Fig. 1) and tunneling is therefore favored. Reached this point, it is interesting to check which are the differences observed with the WKB approach and with the ATM neglecting the contribution of QR. Fig. 2(b) and (c) shows the results for two different reverse bias conditions. As it can be observed, WKB approach strongly overestimates the values of TC for energies near and over $q\phi_B$; in particular, for the energy equal to $q\phi_B$ (0.2 eV) the WKB TC equals 1 while the value predicted by the correct solution of Schrödinger equation is around 0.4 for $V_R = 0.2$ V. ATM without QR gives a TC which is closer to WKB results; however, at high V_R the differences between both models increase [Fig. 2(c)]. For energies over $q\phi_B$, in the thermoionic range, the values of TC with complete ATM are below 1 for all the values of V_R considered. This reduced value of TC is indicative of the importance of QRs. Nevertheless, some tens of millielectronvolts over $q\phi_B$ the transmission coefficient is practically independent on V_R [Fig. 2(a)], which shows that the contribution of QR at very high injection energies is not sensitive to the applied V_R.

The injected current (as a function of the energy) for ATM and WKB approaches is shown in the inset of Fig. 3(a) for two values of V_R. As it can be observed, WKB gives results well over those obtained with the ATM method. The total injected currents for the three models considered are shown in Fig. 3(a); the results including BL due to Schottky effect [13] are also depicted for comparison [Fig. 3(b)]. Let us focus initially on Fig. 3(a). It is interesting to remark that the ratio between the currents obtained with WKB and complete ATM approaches remains rather constant with the applied voltage. The estimated

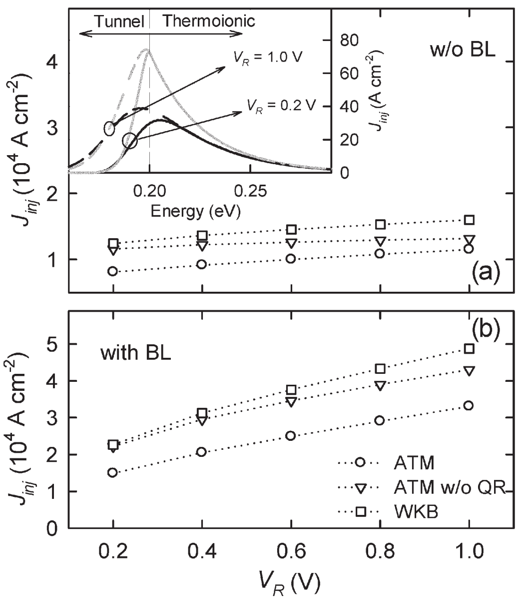

Fig. 3. Injected current densities for the three models considered as a function of V_R without (a) and with (b) BL due to Schottky effect. Inset of Fig. 3(a) shows the injected current density as a function of energy for ATM (black lines) and WKB (gray lines) for $V_R = 0.2$ V (solid lines) and $V_R = 1.0$ V (dashed lines).

error (as compared to the exact solution) induced by WKB approach varies from +53% for $V_R = 0.2$ V to +39% for $V_R = 1.0$ V (although not the subject of this letter, a qualitative similar behavior was obtained if considering higher barrier heights). The reduced error for $V_R = 1.0$ V is due to the fact that–comparatively–tunneling current increases more for ATM approach than for WKB when augmenting V_R. ATM without QR gives results similar to those of WKB at low V_R (since the less sharp is the barrier the closer the WKB solution shall be to an exact solution in which QR are not considered), but ATM without QR current shows a reduced dependence on V_R. BL boosts up the current in all cases, which is due to the significant increase of the thermoionic component; however, once again the ratio between WKB and complete ATM results keeps rather constant when varying V_R. WKB provides an injected current 53% to 47% higher (for $V_R = 0.2$ and 1.0 V, respectively) than ATM. The reduced contribution of tunneling current due to the BL leads to an almost constant error in this case.

IV. Conclusion

A comparison of TC and injected currents calculated using ATM and WKB approaches has been shown. Results indicate that the exact evaluation of quantum transmission through the SB provides a lower TC and consequently reduced current as compared to WKB. Incomplete treatment of quantum reflections in the ATM approach gives also a much higher injected current than if considering the complete ATM solution of Schrödinger equation. The relatively small dependence on V_R of the error induced by WKB (which is practically constant when considering the BL) indicates that WKB could provide a reasonable determination of the total current with a proper consideration of, for instance, Richardson's constant as a fitting parameter.

References

[1] *The International Technology Roadmap for Semiconductors*, 2005, San Jose, CA. [Online]. Available: http://public.itrs.net

[2] E. Dubois and G. Larrieu, "Measurement of low Schottky barrier heights applied to metallic source/drain metal–oxide–semiconductor field effect transistors," *J. Appl. Phys.*, vol. 96, no. 1, pp. 729–737, Jul. 2004.

[3] D. Connelly, C. Faulkner, and D. E. Grupp, "Performance advantage of Schottky source/drain in ultrathin-body silicon-on-insulator and dual-gate CMOS," *IEEE Trans. Electron Devices*, vol. 50, no. 5, pp. 1340–1345, May 2003.

[4] L. Sun, X. Y. Liu, M. Liu, G. Du, and R. Q. Han, "Monte Carlo simulation of Schottky contact with direct tunneling model," *Semicond. Sci. Technol.*, vol. 18, no. 6, pp. 576–581, Jun. 2003.

[5] K. Matsuzawa, K. Uchida, and A. Nishiyama, "A unified simulation of Schottky and ohmic contacts," *IEEE Trans. Electron Devices*, vol. 47, no. 1, pp. 103–108, Jan. 2000.

[6] "New thermionic emission and tunneling models in ATLAS," *Simul. Standard*, vol. 10, no. 8, pp. 6–7, Aug. 1999.

[7] W. W. Lui and M. Fukuma, "Exact solution of the Schrödinger equation across an arbitrary one-dimensional piecewise-linear potential barrier," *J. Appl. Phys.*, vol. 50, no. 5, pp. 1555–1559, Sep. 1986.

[8] K. F. Brennan and C. J. Summers, "Theory of resonant tunneling in a variably spaced multiquantum well structure: An Airy function approach," *J. Appl. Phys.*, vol. 61, no. 2, pp. 614–623, Jan. 1987.

[9] S. Vatannia and G. Gildenblat, "Airy's functions implementation of the transfer-matrix method for resonant tunneling in variably spaced finite superlattices," *IEEE J. Quantum Electron.*, vol. 32, no. 6, pp. 1093–1105, Jun. 1996.

[10] B. Winstead and U. Ravaioli, "Simulation of Schottky barrier MOSFET's with a coupled quantum injection/Monte Carlo technique," *IEEE Trans. Electron Devices*, vol. 47, no. 6, pp. 1241–1246, Jun. 2000.

[11] R. A. Vega, "On the modeling and design of Schottky field-effect transistors," *IEEE Trans. Electron Devices*, vol. 53, no. 4, pp. 866–874, Apr. 2006.

[12] ——, "Comparison study of tunneling models for Schottky field effect transistors and the effect of Schottky barrier lowering," *IEEE Trans. Electron Devices*, vol. 53, no. 7, pp. 1593–1600, Jul. 2006.

[13] S. M. Sze, *Physics of Semiconductor Devices*, 2nd ed. New York: Wiley-Interscience, 1981.

[14] C. Y. Chang and S. M. Sze, "Carrier transport across metal-semiconductor barriers," *Solid State Electron.*, vol. 13, no. 6, pp. 727–740, Jun. 1970.

[15] M. J. Martín, T. González, D. Pardo, and J. E. Velázquez, "Monte Carlo analysis of a Schottky diode with an automatic space-variable charge algorithm," *Semicond. Sci. Technol.*, vol. 11, no. 3, pp. 380–387, Mar. 1996.